Development of a Polyfunctional Dipodal Schiff Base: An Efficient Chelator and a Potential Zinc Sensor

Gupta, Amit; Dangi, Vijay; Baral, Minati*[+]

Department of Chemistry, National Institute of Engineering and Technology Kurukshetra, Haryana-136119, INDIA

Kanungo, B.K.

Department of Chemistry, Sant Longowal Institute of Engineering and Technology, Longowal, Punjab-148106, INDIA

ABSTRACT: *A novel polyfunctional dipodal ligand, L = N,N'-bis[2-[(2-hydroxy-1-naphthyl)methyleneamino]ethyl]propanediamide (DOTA2HNAP) was developed and characterized through elemental and spectral analyses. The complexation behavior of the ligand was investigated with Co^{2+}, Cu^{2+} and Zn^{2+} metal ions by potentiometric and spectrophotometric methods in H_2O-DMSO mixture (99:1) at μ = 0.1M KCl and 25 ± 1 °C. Four protonation constants for –OH of naphtholate groups and –N of imine were determined for the ligand. The ligand forms monomeric complexes of ML type with the metal ions, where coordination occurs through N-imine and O-naphtholate donors (N_2O_2). In the case of a complex of copper, an additional species, MLH_{-2}, was formed due to ionization of the amide groups in a higher pH. The minimum energy structures of the metal complexes in solution have been obtained through molecular modeling studies by using the semi-empirical/ PM3 method. The photophysical properties of DOTA2HNAP were investigated in the presence of a wide range of biologically relevant metal ions. The fluorescence emission of the ligand at 450 nm (λ_{ex} = 361 nm) exhibited a remarkable enhancement with Zn^{2+} ions (1 equivalent) at physiological pH amongst all metal ions. Such behavior enables the ligand to be considered as a suitable model for the detection of Zn^{2+} towards environmental applications.*

KEYWORDS: *Fluorescence spectroscopy; Dipodal chelator; Zn^{2+} Sensor; Potentiometric; Spectrophotometry; Transition metals.*

INTRODUCTION

Transition metal ions such as Co^{2+}, $Cu^{2+}$and Zn^{2+} play a pivotal role in the biological system and are highly required as cofactors for activating various metalloenzymes, regulating neural signal transduction, gene expression, and cellular metabolism [1-3]. Despite their necessity in bio-systems, an excess of these metals fetches various metal overload diseases. Extensive applications of Cu^{2+} in industries particularly in catalytic processes are responsible for posing copper toxicity in the environment as its high exposure to the biological system causes

***** *To whom correspondence should be addressed.*
+ E-mail: minatibritkkr@gmail.com
1021-9986/2019/6/141-156 16/$/6.06

atrophic changes in the nasal mucous membrane, kidney, and liver which leads to Wilson disease in extreme conditions [4]. Similarly, Zn^{2+} from the polluted waste of industries may lead to various health issues as it suppresses the iron and copper absorption and causes nausea, loss of appetite, diarrhea [5]. Further, cobalt toxicity due to rapid exposure of Co^{2+} in the environment affects lungs and eyes causing asthma, poor vision [6] and another related disease. Accordingly, effort needs to be made to develop a tool that can be used for easy detection or sequestration of such essential metal ions in an environment so that their level can be maintained, and environmental toxicity can be avoided.

From last few decades Schiff bases have been drawing attention of the researchers in coordination chemistry, due to their capability of forming stable complexes with metal ions and also, for their high selectivity and sensitivity towards specific metal ions, thus are useful in potentiometric sensing, homogeneous and heterogeneous catalytic processes (such as in polymers, dyes and biological systems) and synthetic enzyme preparations [7]. In medicine and pharmacy, complexes of transition metal ions with Schiff bases have been explored as potent antitumor, antimicrobial, antiviral and antifungal agents [8-10]. The documentation of work based on the determination of protonation constants and stability constants of these molecules in solution are scarce due to their insolubility and possible hydrolysis of the ligand in an aqueous medium. Although much efforts have been imposed in syntheses of such molecules, still there exists vast scope in introducing more novel Schiff bases with improved photophysical properties, binding efficiency, effective coordination behavior with metal ions of industrial or biological relevance. The novelty can be achieved by designing and modulating features of binding moieties with greater suitability. 2-hydroxynaphthaldehyde Schiff bases have gained attention due to their advantages of exhibiting two types of intramolecular H-bonds i.e (N---H-O) and (N-H----O) in the ground state and also, for the properties of photochromism and thermochromism [11]. Such properties pertain with the transfer of a proton between hydroxyl oxygen and imine nitrogen in the excited states forming either enol-imine form (N---H-O) or keto-amine form (N-H---O) [12] , the probability of the existence of either form is dependent on pH and polarity of the solvent. In contrary, the salicylaldehyde based Schiff bases form only N---H-O type of H-bonding which is due to the disruption of π-electron density (aromaticity).

In the above perspective, the present study was designed to develop a novel polyfunctional dipodal Schiff base (DOTA2HNAP), structured with a central unit, spacers of azomethine group carrying pendants of 2- hydroxynapthaldehyde binding moieties, and investigation of its coordination behavior with some metal ions viz., Co^{2+}, $Cu^{2+}$and Zn^{2+}. Also, the photophysical properties of the molecule are investigated in presence of biologically relevant metal ions to explore the ligand's potential use as an optical sensor in the field of environmental and industrial applications.

EXPERIMENTAL SECTION

Materials and measurements

All reagents of ultra pure grade such as malonic ester, ethylenediamine, 2-hydroxynapthaldehyde were purchased from Sigma-Aldrich and were used without further purification unless otherwise stated. Analytical grade solvents methanol, ethyl alcohol, tetrahydrofuran (THF) and others were brought from Fisher Scientific and S.D. Fine Chemicals Ltd. Before using, solvents were dried over suitable drying agents as per standard literature [13]. Melting points were determined on digital melting point apparatus Microsil. Elemental analyses were done on Euro EA 3000, 60 HZ 12000 W analyzer. FT-IR spectrum was obtained in transmission mode with Perkin-Elmer FT-IR spectrometer SPECTRUM 1000 in MID-IR region range (4000-500 cm^{-I}). The ^{1}H and ^{13}C NMR spectra of the ligand were taken on a Bruker Avance-II 400 NMR spectrometer in d_6-DMSO. The chemical shifts were quantified in terms of δ values (ppm). Tetramethylsilane was used as an internal reference. For solubility reason, the ligand was dissolved in H_2O-DMSO mixture of ratio 99:1 (v/v). Solutions were prepared in Millipore grade de-ionized water and weighing of the ligand and metal salts were done on sophisticated electronic balance CAS-CAUW 220D up to a level of four digits. The exact concentration of KOH (0.1M) and HCl (0.1M) were confirmed potentiometrically by acid-base titrations using potassium hydrogen phthalate and oxalic acid (0.1M) as primary standards. Before preparing stock solutions in Millipore grade water, N_2 gas was flushed in continuity to remove CO_2 and O_2.

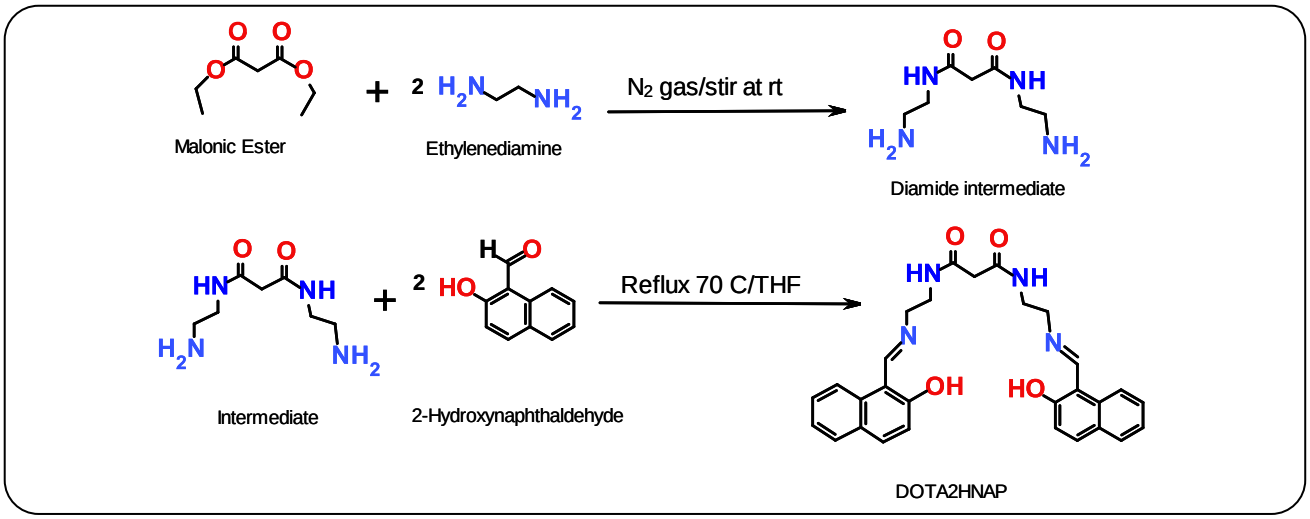

Scheme 1: Synthesis of dipodal ligand DOTA2HNAP.

Synthesis and characterization of DOTA2HNAP

The synthesis of dipodal chelator DOTA2HNAP was done as shown in scheme 1. In the first step, 16.0 g distilled malonic ester (0.1 mmol) was added gradually to 30.0 g freshly distilled ethylenediamine (0.5 mmol) into a three-neck flask and stirred at room temperature for 7 days under N_2 atmosphere. An off-white colored residue of malonamide intermediate was obtained on treatment with cold dry methanol which was filtered off, washed with cold dry methanol and dried in vacuum. The compound is completely soluble in water and the melting point was noted in the range 210 - 214 °C.

In second step, 0.26 g (0.00138 mmol) of the intermediate compound was dissolved in hot dry ethanol (10 ml) and was added drop wise to the stirred solution of 1.3 g (0.0076 mmol) 2-hydroxynaphthaldehyde in 30.0 mL of dry ethanol. The resulted solution was refluxed for 3h while a brown solid **1** was separated out, filtered off and washed thoroughly with THF/MeOH mixture and dried in vacuum which afforded 0.206 g , 79.4%, M.p.: 163-165 °C; ^{1}H-NMR (400 MHz, dmso d_6, 25 ºC, TMS): δ = 3.0 (t, 4H,C**H**$_2$), 3.1 (t, 4H, C**H**$_2$), 3.7 (s, 2H, C**H**$_2$), 6.7- 8.3 (m, 12H, **H**-aromatic), 9.0 (d, 2H, -C**H**=N-), 14.0 (s, 2H, -CH-N**H**-) ppm; ^{13}C-NMR (400 MHz, dmso d_6, TMS): δ = 43.2 (-**C**H$_2$), 50.2 (-**C**H$_2$), 99.4 (-**C**H$_2$), 105.8 - 136.9 (-Ar-**C**), 159.7 (-NH-**C**H=), 167.2 (-NH-**C**=O), 176.9 (-**C**=O keto form) ppm; IR (KBr): $\bar{\nu}_{max/cm^{-1}}$ = 3418 (-OH), 3283 (-NH), 3063 (-CH,Aromatic), 1683 (-C=O), 1639 (-C=N), calculated for ($C_{29}H_{28}N_4O_4$): C, 70.1; H, 5.7; N, 11.13; found: C, 70.8; H, 5.9; N, 11.4.

Potentiometric titration

The protonation constants of the ligand and formation constants of the metal complexes were determined potentiometrically at temperature 25 ± 1 ºC, maintained in a double wall glass jacketed titration cell connected to a constant temperature circulatory bath. The Thermo Scientific Orion Star A111 pH meter accompanied with Ross Ultra combination pH electrode 8102BNUWP was used for pH measurements. The observed pH was measured as –log [H^+]. The calibration of the electrode was done by the classical method to read the pH accurately and precisely [14]. Moreover, titrations were done using auto-pipette (0.5 ml, least count 0.01mL) for adding lesser volume. A stock solution of HCl (0.1M) was titrated against standard KOH (0.1M).

As the ligand shows solubility problem in an aqueous medium at higher concentration i.e 10^{-3}M, the more diluted solution was preferred for the potentiometric studies. The ligand solution (1x 10^{-5}M) made in H_2O:DMSO 99:1 mixture was acidified up to pH 2.0 by using 0.1M HCl acid and the resultant solution was titrated against 0.1M KOH solution in pH range 2 - 11 at μ = 0.1M KCl and temperature 25 ± 1 ºC to determine the protonation constants. Complexation behavior of the ligand was explored with divalent metal ions viz., Co^{2+}, $Cu^{2+}$and Zn^{2+} by titrating metal-ligand solution (1:1,40 mL) against 0.1 M KOH solution. Formation constants (log β) of the metal complexes and protonation constants of the ligand were determined by using non-linear least square refinement program Hyperquad 2006 [15],

and Hyss 2009 was used for the plot of species distribution curves [16].

Spectrophotometric and Fluorescence measurements

Electronic absorption spectra were recorded on Thermo Scientific Evolution 201 UV-Visible Spectrophotometer using 1.0 cm path length quartz cuvette, externally connected to HEWLETT PACKARD Intel Core 2 duo computer. Spectrophotometric titration of a 40 ml H_2O-DMSO (99:1, v/v) solution of DOTA2HNAP (4 x 10^{-5} M) was acidified by adding 0.1M HCl and ionic strength was maintained by adding 2.5 ml of 0.1M KCl. The resulted solution was titrated against freshly prepared standardized 0.1M KOH solution in pH range 2.0-8.5. During spectrophotometric titration, thermostat glass jacketed vessel was used to maintain the temperature 25 ± 1 ºC throughout the experiment. After each addition of a base, sufficient time was allowed to ensure equilibrium before pH measurement and spectrum analysis. For the complexation studies of the ligand, solutions of 4 x 10^{-5} M concentration of the ligand and metal ions were used. The formation constants from spectral data were calculated by using a nonlinear least square fitting program, HYPSPEC [15].

Fluorescence spectra were recorded using Agilent Fluorescence Spectrophotometer with 1.0 cm path length quartz cuvette, externally connected to HEWLETT PACKARD Intel Core 2 duo computer. The emission spectra of the ligand (L) were studied with excitation wavelength, λ_{ex} = 361 nm, slit width 10 nm at varied concentrations and pH range 2 to 8.5. Also, fluorescence behavior was investigated in the presence of wide range of metal ions viz., Na^+, K^+, Ca^{2+}, Mg^{2+}, Zn^{2+}, Co^{2+}, Pb^{2+}, Cu^{2+}, Al^{3+}, Cr^{3+} at pH 7.4 ± 0.1 using HEPES buffer. The effect of increasing concentration of Zn^{2+} (0 to 60 µM) on the fluorescence intensity of the ligand (40 µM) was studied in the same pH.

The detection limit of the ligand for the Zn^{2+} ions was calculated from the fluorescence titration at pH (7.4) as per the definition by IUPAC i.e. 3.3*SD/m [18], where 'SD' is the standard deviation of the fluorescence intensity of the blank (ligand only) and 'm' is the slope of the calibration curve constructed between fluorescence intensity of ligand (40µM) and the micromolar concentration of Zn^{2+} ions at 450 nm.

Computational methods

A Pentium dual-core CPU T2370 machine with Window 7 environment was used for all calculations. The minimum strain energy of the ligand DOTA2HNAP was achieved by molecular mechanics using MM+ force field followed by PM3 quadratically convergent self-consistent fields (SCF) method at Restricted Hartree-Fock (RHF) level using Hyperchem7.5.

Steepest descent method followed by Polak-Ribiere was taken for geometry optimization with convergence limit 0.0001 kcal/mol and RMS gradient 0.001 kcal/mol. The obtained structures were reoptimized by the semiempirical/PM6 method. The infrared and electronic spectra of DOTA2HNAP was calculated through the semi-empirical method using PM6 and ZINDO/S Hamiltonian parameters using CAChe software respectively.

RESULTS AND DISCUSSION

Design, synthesis and characterization of DOTA2HNAP

The new polydentate chelator DOTA2HNAP was designed taking diethyl malonate as a central unit, diaminoethane as spacers offering two binding moieties (–C=N- of imine and –OH of naphthol ring) and link to the central unit through amide groups. The binding efficiency of the dipodal ligand, towards divalent metal ions viz., Co^{2+}, Cu^{2+} and Zn^{2+} are expected to favor greatly due to its structural design that allows the flexible pendant arms to arrange themselves in a way to provide an appropriate cavity to fit well with the metal ions.

The compound was synthesized with a reasonable yield (~79 %) in two steps as described in Scheme 1. Malonic ester and diaminoethane were reacted in N_2 atmosphere at room temperature to give a water-soluble malonamide intermediate which on condensation with 2-hydroxynaphthaldehyde gave a brown solid, DOTA2HNAP. The compound is completely soluble in DMSO and partially soluble in THF/ethanol/chloroform. The FT-IR spectrum recorded on KBr pellet showed a broad band at 3418 cm^{-1} that can be assigned to the -OH vibrational frequency which usually appears at ~ 3730-3520 cm^{-1} [19]. The shifting of ν_{OH} may be attributed to the presence of intramolecular H-bonding between –OH and -C=N. The appearance of an additional band at ~3283 cm^{-1} due to ν_{NH} confirmed the presence of amide linkage. The sharp peaks at 1639 cm^{-1} and 1683 cm^{-1}

were attributed to the $\nu_{C=N}$ and $\nu_{C=O}$ respectively. Besides, peaks obtained at 1543 cm^{-1} and at 3063 cm^{-1} are due to (-NH-) bending and ν_{C-H} (aromatic) respectively. The theoretical IR spectrum calculated by the semi-empirical method using PM6 parameters also showed the closest agreement in terms of the pattern of peaks with the experimental ones, and confirmed the assignments as shown in Fig. S1.

The ^{1}H NMR spectrum (Fig. S2) showed a peak at 3.7 ppm (singlet, 2H) corresponding to the active methylene group of the central unit, while two triplets obtained at 3.0 ppm and 3.1 ppm, are due to the methylene groups attached to the amide and imine groups, respectively. A doublet was found at 9.0 ppm due to the imine proton (–C**H**=N-). Peaks in the range of 6.7 – 8.0 ppm were attributed to the aromatic protons. The peaks for amide protons (-CO-N**H**-) was not observed due to merging with the peaks of aromatic protons, similar are also reported in the literature [20]. The peak at 14.0 ppm (singlet, 2H) corresponds to the proton of –N**H**-CH=, which is the characteristic marker of the existence of the keto-imine form in a polar solvent.

The ^{13}C NMR spectrum also confirmed the formation of a keto-imine isomeric form of the ligand, as the peak at 176.9 ppm attributed to the aromatic ring carbon when exists in a keto form. This demonstrates a significant parameter about the proton transfer process between –**O**H of naphthol ring and –**N**=C- of imine group. Occurrence of keto-imine form in polar solvents has also been documented by Sosa et al., where it is reported that in the polar solvents, 2-hydroxynaphthaldehyde based Schiff bases exist mainly as –NH tautomer because of polar solvents which are known to promote proton transfer process by stabilizing the keto-amine form and thus, favoring the tautomerization process[21]. Peaks obtained in range 105.8 - 136.9 ppm correspond to the carbons of naphthyl ring. The chemical shift at 159.7 ppm indicates the carbon of –NH-**C**H= group (keto-form). The peaks at 43.2, 50.2 and 99.4 ppm attribute the presence of three methylene groups of DOTA2HNAP. The –**C**H_2- of the central unit is the most de-shielded methylene group (99.4 ppm) among all methylene groups due to the presence of two electron withdrawing neighbors in the vicinity as shown in the Fig. S3.

The electronic absorption spectrum of DOTA2HNAP showed three bands at 252, 320 and 361 nm, the first two are due to $\pi\rightarrow\pi^*$ transition of the ring and the third one represents to the $n\rightarrow\pi^*$ transition of the imine group. Theoretical electronic absorption spectrum obtained by using semi-empirical ZINDO/s method followed the same trend confirming the assignments. The experimental and theoretical absorption spectrum has been illustrated at Fig. S4.

Ligand Protonation Constants

The protonation constants of DOTA2HNAP were evaluated by combined use of potentiometric and spectrophotometric titrations in pH range 2 - 11. Due to the solubility problem, studies were conducted in H_2O-DMSO 99:1 (v/v) mixture. During potentiometric studies, the ligand solution was titrated against 0.1M KOH at ionic strength 0.1M KCl and 25 ± 1 ºC. The potentiometric curve of the ligand showed two inflection points at 'a' = 2 and 4 (moles of base used) as shown in Fig. 1. Value a = 2 represents neutralization of excess acid, while a = 6 indicates release of four protons from the ligand. Further, the protonation behavior of the dipodal Schiff base DOTA2HNAP was illustrated through the refinement process in the best fit model whereas only four protonation constants could be determined with equilibrium reaction as shown in Eq. (1).

$$[LH_{n-1}]+[H] \rightleftharpoons LH_n \quad (1)$$

$$K_{1n} = \frac{[LH_n]}{[LH_{n-1}]+[H]}$$

For the ligand, there exists a total of six protonation sites; two each counting for amide, imine and –OH groups (aromatic ring). However, only four protonation constants (log K) could be determined in the adopted experimental conditions and are given in Table 1. The amide groups could not be deprotonated within the experimental pH range 2 – 11, as they require a highly basic condition [20]. The first two protonation constants obtained were assigned to two naphtholate oxygens and latter two to the imine nitrogens (-C=N-). Such assignments are ascribed due to the fact of high basicity of naphtholate oxygen as compared to weak base imine group [22]. The log K values determined for the ring –OH group are found to be less than the naphthol group, which is due to the presence of intramolecular H-bonding between imine nitrogen (deprotonated) and hydroxy group of the aromatic ring. Moreover, the protonation

Table 1: Protonation constants (log K) of DOTA2HNAP 25 ± 1 ºC and μ = 0.1 M KCl, (A = potentiometry and B = Spectrophotometry).

Equilibrium	log K		Protonation sites
	A	B	
$L + H \rightleftharpoons LH_1$	8.78 ± 0.03	8.84 ± 0.01	$-O^-$ (aromatic)
$LH_1 + H \rightleftharpoons LH_2$	7.42 ± 0.01	7.64 ± 0.04	$-O^-$ (aromatic)
$LH_2 + H \rightleftharpoons LH_3$	3.34 ± 0.02	3.65 ± 0.03	=N- (imine)
$LH_3 + H \rightleftharpoons LH_4$	1.23 ± 0.03	1.38 ± 0.02	=N- (imine)
$L \rightleftharpoons LH_{-1} + H$	-7.80 ± 0.04	-7.30 ± 0.01	
$LH_{-1} \rightleftharpoons LH_{-2} + H$	-8.03 ± 0.01	-8.09 ± 0.03	
$LH_{-2} \rightleftharpoons LH_{-3} + H$	-9.28 ± 0.02	-9.15 ± 0.03	
$LH_{-3} \rightleftharpoons LH_{-4} + H$	-10.36 ± 0.03	-10.12 ± 0.04	

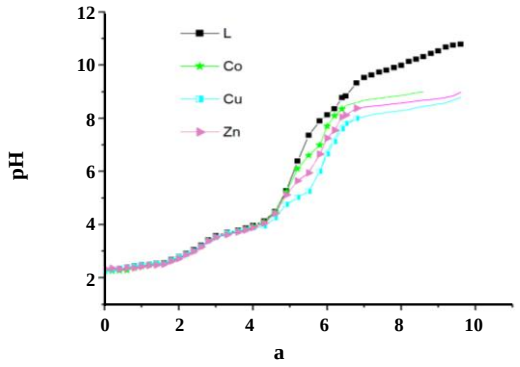

Fig. 1: Potentiometric titration curves of the dipod DOTA2HNAP between pH versus 'a' (moles of base added per mole of the ligand) in the presence of the metal ions Co^{2+}, $Cu^{2+}$and Zn^{2+} in 1:1 metal-ligand ratio ●, [M] = [L] = 1 x 10^{-5}M at μ = 0.1M KCl and T = 25 ± 1 ºC ●, Dash lines: appearance of turbidity or solid phase in the solution during titration.

constants K_3 and K_4 corresponding to imine groups were lower than that of –OH (ring). This can be attributed to the fact that the imine group which is present in conjugation with 2-hydroxynaphthaldehyde group has the reduced electron density causing for low protonation constant. The values generally lie in pH range 1-3. Similar observations were also recorded [22] in determination of protonation constants of imine groups, present in conjugation with some other electron withdrawing moieties in pH range 2-11.

The experimental curve did not give a complete match with the theoretical curve particularly at higher pH range (i.e., > 8.5) when a model with only four protonation constants was taken into account but, after inclusion of four hydrolyzed species viz., LH_{-1}, LH_{-2}, LH_{-3} and LH_{-4} in the model, the refinement process gave the best fit to the experimental curve which indicates occurrence of hydrolysis in the ligand at pH > 8.5. Schiff bases are not stable under basic conditions due to the partial hydrolysis at imine linkage (-C=N-) [23] as shown in the mechanism (Fig. 2), from which it is assumed that four protons are released during hydrolysis per molecule of the ligand.

Formation of various protonated as well as hydrolyzed species is pH dependent and is depicted in species distribution diagram (Fig. 3a). From the diagram it is evident that DOTA2HNAP is stable to hydrolysis up to pH ~ 8.5 and beyond this pH, it gets hydrolyzed giving LH_{-n} (n = 1, 2, 3, 4) species. In pH 2–3, deprotonation of the ligand leads to the formation of LH_3 species by 73.0%. Further increase in pH, causes the formation of diprotic species LH_2 which remains stable up to pH ~ 5.7. Subsequently, LH and L^{2-} species are formed at pH ~7.8 and ~8.2, with a maximum percentage of formation 67.0 and 16.0 respectively. A further rise in pH causes the formation of hydrolyzed species LH_{-1}, LH_{-2} and LH_{-3} between pH ~ 8.2 - 10 and after pH > 10, LH_{-4} species becomes more predominant.

The electronic transition spectra of the ligand were recorded in the region 240 nm to 500 nm in pH range 2–8 (Fig. 3b). The formation of isosbestic points implicates the presence of equilibrium between protonated and deprotonated forms of the ligand. Formation of the protonated (LH_1, LH_2, LH_3 and LH_4) and hydrolyzed

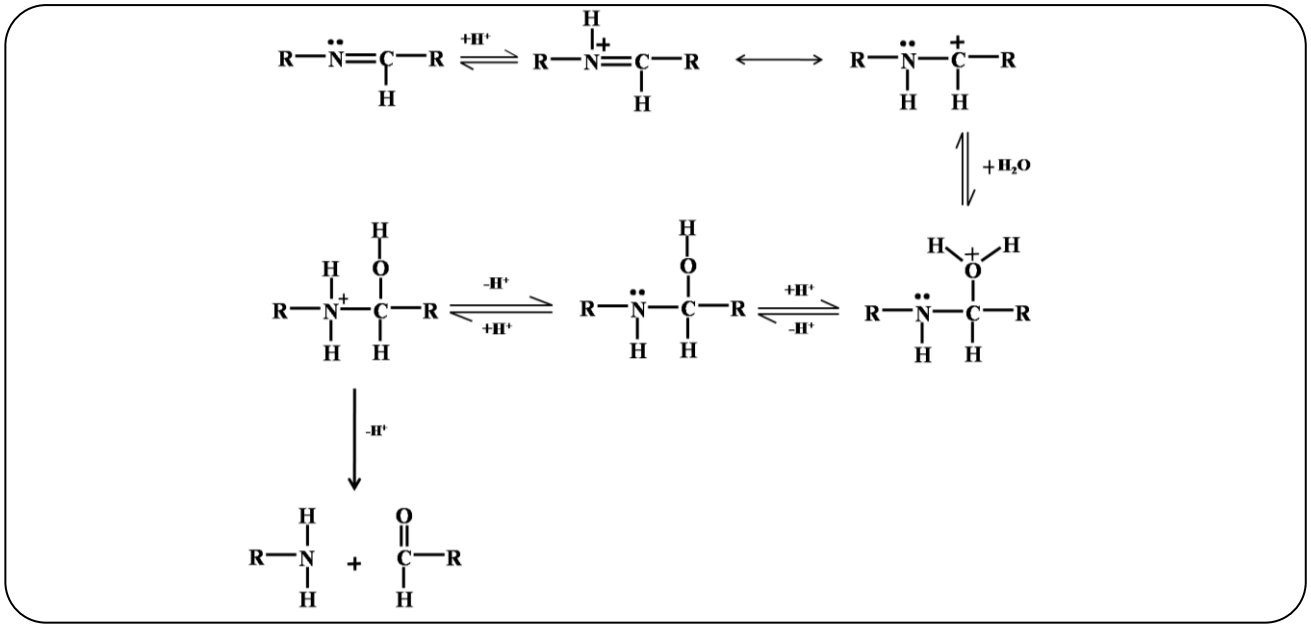

Fig. 2: Hydrolysis of Schiff base in basic medium.

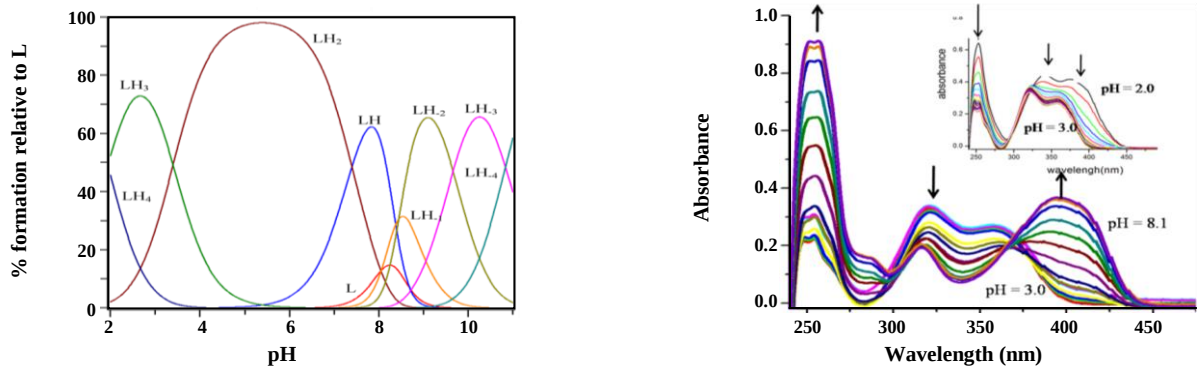

Fig. 3: (a) pH dependent distribution of the species of DOTA2HNAP ● (b) Electronic spectra of DOTA2HNAP as a function of pH (3.0 – 8.1) and (2.0 to 3.0) (inset) respectively during spectrophotometric titrations where [DOTA2HNAP] = 4 x 10^{-5}M, at μ = 0.1M KCl and T = 25 ± 1 ºC.

species (LH_{-1}, LH_{-2}, LH_{-3} and LH_{-4}) were also established after analysis of experimental data by global fitting of the whole spectra through a non-linear least square fitting program HYPSPEC.

The electronic absorption spectra of the ligand showed three bands at 252, 340 and 376 nm corresponding to π→ π* (first two bands) and n→ π* (third band) transitions at pH ~ 2. On increasing the pH to 3, all three bands showed the hypochromic effect and a concomitant shift in the absorbance observed for the last two bands (320 and 361 nm) as shown in Fig. 3b (inset), which can be explained due to the existence of an equilibrium between the keto and enol forms at low pH, where keto form is a dominant one. However, on further rise of pH (> 6), the intensity of the absorbance at λ = 252 nm increases whereas the intensity at λ = 320 nm decreases.

The band obtained at 361 nm shifted to longer wavelength (391 nm) with a concomitant rise in the absorbance intensity. These observations can be justified on the basis of deprotonation of the hydroxyl group of naphthalene ring (formation of naphtholate ions) which stabilizes π* excited state by charge delocalization and hence decreases the energy gap between lower excited state and higher ground state. Besides, conjugation between the imine group and naphthyl ring influences the energy of transition and attributed to redshift for

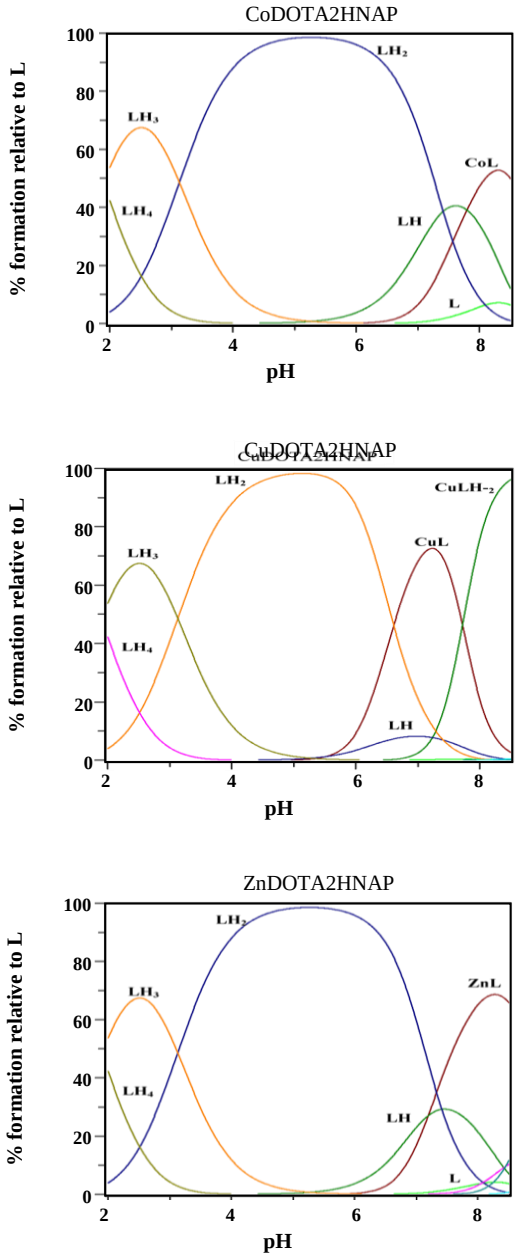

Fig. 4: Speciation diagram (% formation vs pH) calculated for 1:1 (a) Co^{2+}, (b) $Cu^{2+}$and (c) Zn^{2+}.

the imine band. The experimental values obtained through spectrophotometric studies are in accordance with those obtained through potentiometric method.

Metal-Ligand Complex Formation

Complexation behavior of the ligand with the divalent metal ions viz., Co^{2+}, $Cu^{2+}$and Zn^{2+} was studied by potentiometric and spectrophotometric methods, and formation constants of the metal complexes were determined. The potentiometric curves of M-L complex (1 : 1) for all the divalent ions are as shown in Fig. 1. The deviation of the M-L titration curves from the ligand alone at pH~5 for Cu^{2+}, and at pH~6.0 for Zn^{2+} and Co^{2+}, indicates the coordination of the ligand with the metal ions. The data between pH ~ 8 - 8.5 for all metal-ligand titrations were not taken for the calculation due to the appearance of turbidity. Various metal-ligand species were formed during complexation at different pH conditions which were established through comutational calculations by using the program HYPERQUAD 2006, and their formation constants were tabulated in Table 2. Inclusion of ML type of the species in the model for all the metal ions, Co^{2+}, Cu^{2+} along with an additional species MLH_{-2}, only in the case of Cu^{2+}, gave a complete match to the experimental curve. Various species existed in the equilibrium can be represented by the following equations:

$$M + L \rightleftharpoons ML \qquad \log\beta_{110} = [ML]/[M][L] \qquad (2)$$

$$M + L \rightleftharpoons ML\,H_{-2} \qquad (3)$$

$$\log\beta_{11-2} = [MLH_{-2}][H^+]^2 / [M][L]$$

From the species distribution diagrams (Fig. 4) it is evident that ML type complexes were formed with a maximum percentage of formation 52, 73 and 62 for Co^{2+}, $Cu^{2+}$and Zn^{2+} respectively. Complexation of the dipodal ligand with the metal ions occurs through two tertiary nitrogens (imine groups) and two naphtholate oxygen donors, forming ML type species. However, the interaction of DOTA2HNAP with Cu^{2+}ions around pH 8, made deprotonation of amide protons feasible the with the formation of MLH_{-2} species. Although amide has a poor binding affinity towards transition metal ions, deprotonation of amide protons in the presence of Cu^{2+} metal ions is well documented [24]. Here the deprotonation is an endothermic process, and such process is not feasible in case of Zn^{2+} and Co^{2+} because the complexes stabilization does not occur with much profit from ligand effects as observed in case of Cu^{2+}.

Coordination behavior of DOTA2HNAP with the above said metal ions was also studied by the spectrophotometric method to ensure the possible

Table 2: Formation constants (log β) of DOTA2HNAP at 25 ± 1 °C and μ = 0.1 M KCl (A= potentiometry and B = spectrophotometry) in aqueous medium.

	log β		
	A	B	Ref
$Co + L \rightleftharpoons CoL$	6.46 ± 0.04	6.86 ±0.02	25
$Cu + L \rightleftharpoons CuL$	7.95 ± 0.02	7.99 ±0.03	20
$Cu + L \rightleftharpoons CuLH_{-2} + 2H$	- 6.80 ± 0.05	-6.95±0.01	26
$Zn + L \rightleftharpoons ZnL$	6.82± 0.03	6.98±0.02	27

coordination modes in the solution. The studies were carried out in 1:1 ligand to metal ratio, [L]=[M]= 4 x10^{-5} M with increasing pH between 2-8, where at pH ~8.5, the solution became turbid. Fig. 5 depicts the molecular absorption spectra of L - M(II) systems. Formation of isosbestic points due to shifting of bands can be observed with the progressive increase in pH. In pH range 2 – 3, the pattern of the absorption spectra of the ligand in presence of the metal ions remains similar to the absorption spectra of the ligand alone, which indicates about the deprotonation of imine group of the ligand in the aforesaid pH range. On increasing the pH above 5, for Cu(II)-L system, the ligand characteristic band at 252 nm ($\pi \rightarrow \pi^*$ transition) experienced slight shift towards longer wavelength along.with a hyperchromic effect. Also, a new band of low intensity had appeared at 288 nm. In the presence of Cu^{2+} ions, absorption bands of the ligand at λ = 320 nm ($\pi \rightarrow \pi^*$ transition) showed a hypochromic shift whereas, band at λ=361 nm ($n \rightarrow \pi^*$ transition) experienced a bathochromic shift. Formation of isosbestic points at 298, 314, 371 and 378 nm implies the involvement of equilibrium between protonated and deprotonated forms of the ligand. No additional bands at higher wavelength were noticed which was due to very low concentration of the solutions. Similar kind of variations were observed in the absorption spectra of the ligand in the presence of other two metal ions (Co^{2+} and Zn^{2+}) in the same pH range suggesting for a similar mode of complexation. The best fit model was obtained with the formation of ML species with all the three metal ions along with the formation of an extra MLH_{-2} species for Cu(II)-L complex. The formation constants for all three metal ions have been tabulated in Table 2. Formation constants of some analogous ligands are presented in Table 3 for comparison.

Fluorescence behavior of the ligand in solution

The multifunctional chelator, DOTA2HNAP at 10^{-5}M concentration showed a weak fluorescence emission at 450 nm when was excited at 361 nm. Fluorescence property of a compound is influenced by various complex processes such as photoinduced Excited State Intramolecular Proton Transfer (ESIPT), Photo-Induced Electron Transfer (PET), and Intermolecular or Intramolecular Charge Transfer (ICT) [28]. Organic molecules possessing proton-donor and proton-acceptor moieties in immediacy like naphthalene group favor ESIPT mechanism facilitated by an intramolecular H-bonding, and provides an ideal component for developing fluorescence assisted sensing molecule [29]. In the present ligand, hydroxynaphthaldehyde ring incorporated with azomethine groups forms intramolecular H-bonding which allows protons transfer from –OH group (aromatic ring) to nitrogen (imino group) in the excited (π - π^*) state through an ESIPT process (Fig. 6). In the excited state, fast decaying enol state is converted into the cis-keto tautomer, which is responsible for shorter fluorescence lifetimes through steady-state emission [30]. In addition to ESIPT, there can be other plausible mechanisms such as isomerization at –C=N bond and PET which are associated with the weak fluorescence in the similar structured Schiff bases [31-32].

The fluorescence behavior of the ligand was analyzed at different concentration and pH (Fig. 7). It was observed that the fluorescence intensity of the neutral ligand decreases in its protonated and deprotonated form, which might be for the higher probability of formation of the keto form in low pH (~ 2) due to the arrested charge density of imine nitrogen by the protons. Also, at higher pH the decrease in fluorescence intensity

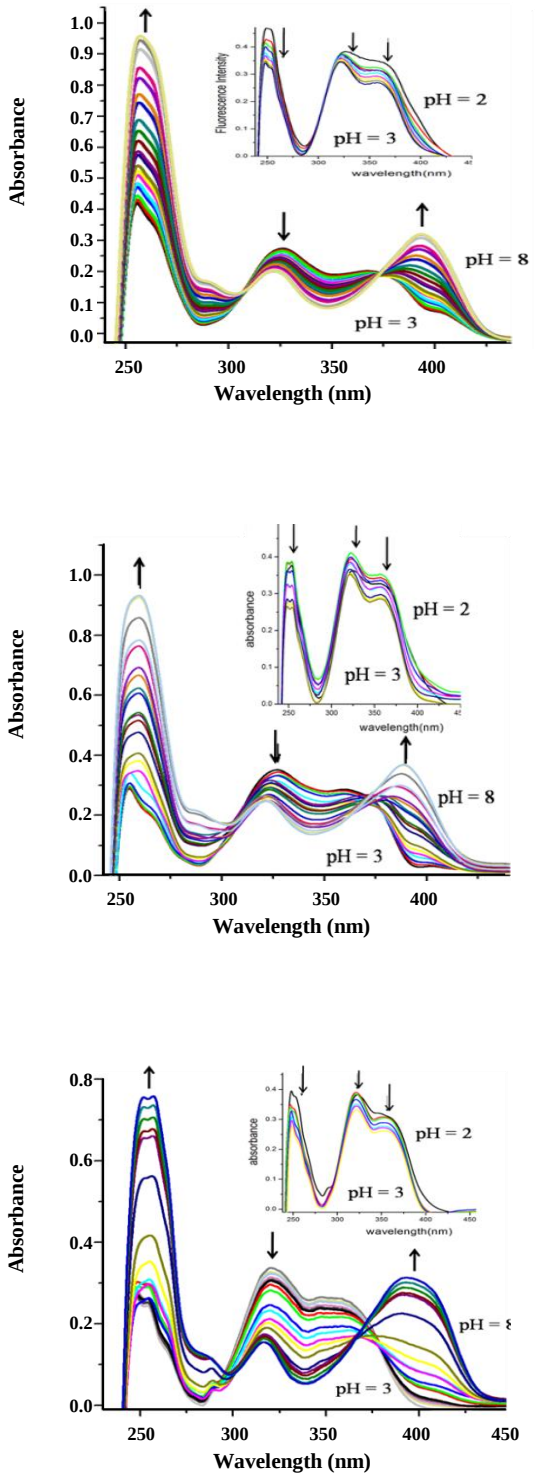

Fig. 5: Electronic spectra of DOTA2HNAP as a function of pH during spectrometric titration with [M] = 4 x 10^{-5} M where [M] = Co^{2+} (a), Cu^{2+} (b) and Zn^{2+} (c) and [L] = 4 x 10^{-5} M in H_2O-DMSO (99:1, v/v) mixture at μ= 0.1 M KCl at T = 25 ± 1 °C.

can be explained due to the occurrence of PET or favored isomerization [33].

Fluorescence behavior of metal-ligand complexion solution

The transition metal ions in the vicinity of fluorophore may alter the photophysical properties resulting in modulated oxidation potential of the donor group which attributes to enhancement or quenching [32-37] in the fluorescence intensity. The dipod showed significant enhancement in fluorescence intensity in pH range 6.8–8.0 in presence of Zn^{2+} ions. No major changes except a slight reduction in fluorescence emission of the ligand were observed with Co^{2+} and Cu^{2+} ions. The fluorescence behavior of the ligand-Zn^{2+} system was further studied in pH 7.4, on account of its physiological importance for wider applications (Fig. 8).

The effect of metal ions M(II) = Co^{2+}, $Cu^{2+}$and Zn^{2+} on the fluorescence emission spectra of DOTA2HNAP in H_2O-DMSO (99:1, v/v) at pH 7.4 is shown in Fig. 9. Upon addition of Zn^{2+} to the ligand solution, there was a large improvement in fluorescence emission exhibiting blue shift of ~ 18nm. Most plausibly, the observed enhancement in fluorescence intensity with Zn^{2+} at a neutral pH is due to the arrested isomerization of –C=N- group in the excited state of the ligand. Zn^{2+} being a photo physically inactive and spectroscopically silent due to filled d-orbitals (d^{10}), also follows large chelation-enhanced fluorescence (CHEF) effect, in comparison to other metal ions, consequently, Zn-L does not display any electron transfer and energy transfer processes [39]. Moreover, such unique selectivity of various ligands including Schiff bases towards Zn^{2+}has been well reported [31]. The possible explanation for the negligible reduction of fluorescence intensity of the ligand on coordination with Co^{2+} and Cu^{2+} can be attributed to the ligand to metal (L→M) charge transfer due to the presence of empty d-orbitals [40]. The reduction in fluorescence emission beyond pH > 8, could be due to the precipitation in the solution mixture at high basic condition.

The effect of increasing concentration of Zn^{2+} ions on fluorescence emission of the ligand ([L]=40 μM) was investigated where, the maximum enhancement in the fluorescence intensity was observed with 1 mole equivalent of Zn^{2+} (Fig. 10). The detection limit of the Zn^{2+} was found to be 8.4 x 10^{-6} M.

Table 3: Comparison of the formation constants (log β) between DOTA2HNAP and other similar dipodal metal complexes of Co^{2+}, Cu^{2+} and Zn^{2+} ions.

S.No	Ligand	Structure	Log β		
			Co^{2+}	Cu^{2+}	Zn^{2+}
1	DOTA2HNAP	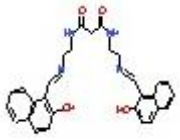	6.46	7.95	6.82
2	2-hydroxy naphthaldehyde Schiffbase	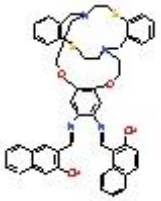	4.22[a]	___	4.87[a]
3	BHAEM	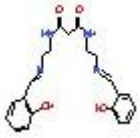	4.67[b]	6.86[b]	4.8[b]
4	N,N'-bis(salicylidene)-1,4-diminobutane	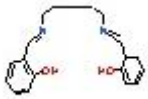	____	3.58[c]	3.35[c]
5	H_2BHBDAE	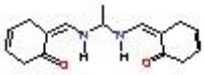	3.43[d]	4.87[d]	3.12[d]

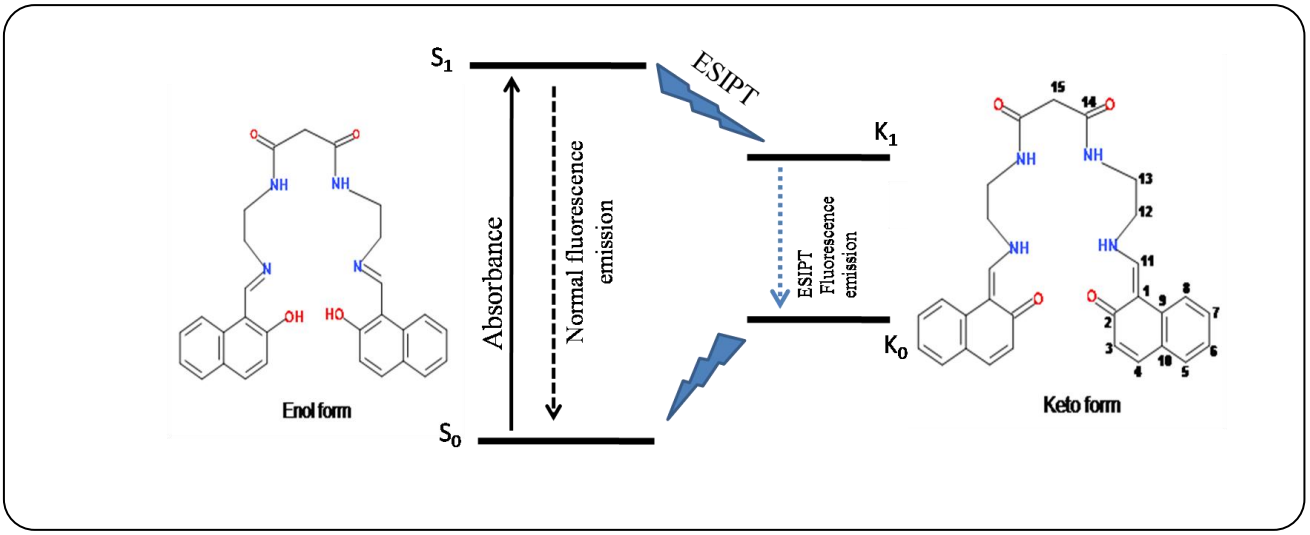

Fig. 6 Principle photophysics of ESIPT (where excitation occurs from S_0 to S_1 state of enol form of the ligand followed by relaxation of the cis-keto form from K_1 to K_0 attributing to a longer wavelength fluorescence emission.)

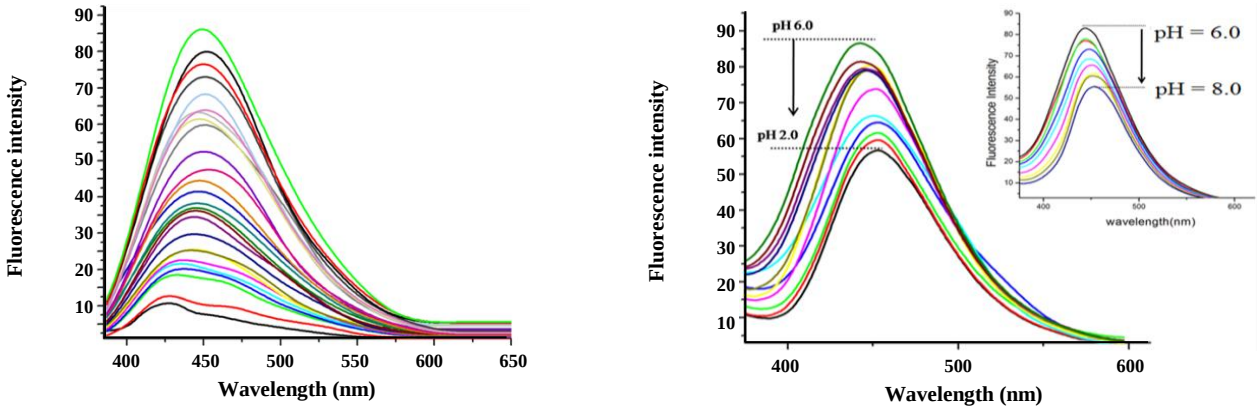

Fig. 7: (a) Fluorescence spectra of ligand with varying concentration (5 x 10^{-8} to 10^{-5}M,) from bottom to top) ● (b) Fluorescence spectra of ligand at varying pH 6 – 2 (in inset pH 6 – 8) at λ_{Ex} = 361 nm and λ_{Em} = 450 nm; slit width = 10 nm.

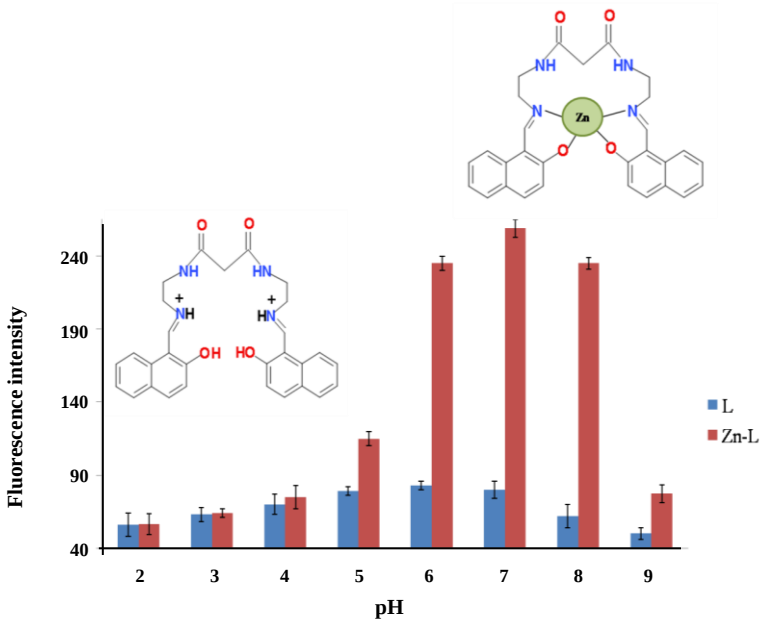

Fig. 8: pH-dependent fluorescence intensities of DOTA2HNAP in the absence and presence Zn^{2+} in pH range 2.0 to 8.5 at λ_{ex} = 361nm; [L] = 4 x 10^{-5} M and [Zn^{2+}] = 4 x 10^{-5}M; slit width = 10nm.

Interesting fluorescence behavior of the ligand (L) in presence of Zn^{2+} prompted us for its selectivity studies, where the ligand [L]= 40 µM was investigated with different essential metal ions such as K^+, Na^+, Ag^+, Ca^{2+}, Mg^{2+}, Mn^{2+}, Co^{2+}, Hg^{2+}, Pb^{+2} , Cu^{2+}, Fe^{3+} and Cr^{3+} (Fig. 11). None of them brought any significant change in the fluorescence of the ligand. However, with Fe^{3+} ions, a significant quenching in the ligand's fluorescence intensity was observed, hence, providing a scope for future studies on the photophysical behavior of the ligand with Fe^{3+} ions.

Molecular Modeling

Molecular modeling studies have been investigated on DOTA2HNAP and its complexes with Co^{2+}, Cu^{2+} and Zn^{2+}. The PM6 optimized molecular structures of all three metal-ligand complexes are shown in Fig. 12, where the ligand coordinates to the metal ions M^{2+} through O and N donor atoms. The geometry of the metal-ligand complexes with four and six coordination numbers were evaluated by optimizing each complex species. The minimum energy structures were the hexacoordinated ones with four coordination sites occupied by the

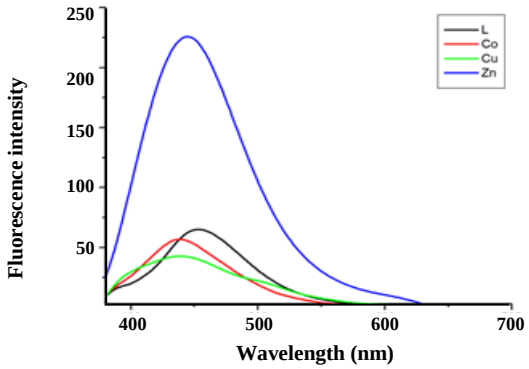

Fig. 9: Fluorescence spectra of ligand in the absence and presence of metal ions M = [Co^{2+}, $Cu^{2+}$and Zn^{2+}] at λ_{ex} = 361nm; pH = 7.4; [L] = 4 x 10^{-5} M and [M] = 4 x 10^{-5}M; slit width = 10nm.

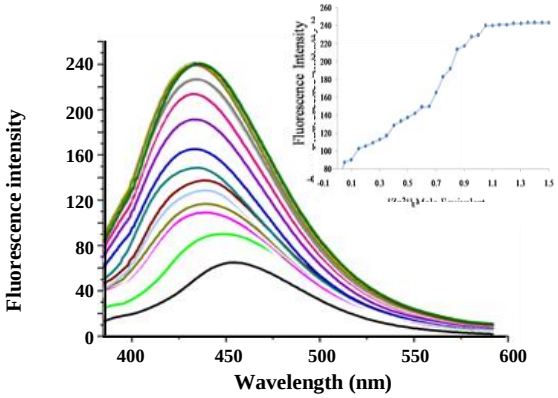

Fig. 10: Fluorescence spectra of ligand [L] = 40µM as a function of externally added [Zn^{2+}]. From bottom to top [Zn^{2+}] = 0, 4, 8, 12, 16, 20, 24, 28, 32, 36, 40, 44, 48, 52, 56 and 60µM in H_2O-DMSO (99:1, v/v); (insert represents the fluorescence intensity of [L] as a function of mole equivalent of [Zn^{2+}] added externally; λ_{Ex} = 361nm

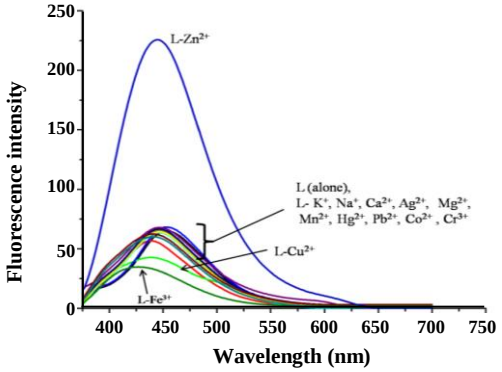

Fig. 11: Fluorescence spectra of DOTA2HNAP (40µM), DOTA2HNAP + M^{n+} (40µM), where M^{n+} = K^+, Na^+, Ag^+, Ca^{2+}, Mg^{2+}, Mn^{2+}, Co^{2+}, Hg^{2+}, Pb^{+2}, Cu^{2+}, Fe^{3+}, $Cr^{3+}$and Zn^{2+} at λ_{Ex} = 361nm.

tetradentate ligand. The proposed six-coordination structures with two water molecules were rejected by the minimization program. The simulated metal complexes structures of Zn^{2+} and Co^{2+} with the ligand showed tetrahedral geometries whereas Cu^{2+} ligand complex was found exhibiting square planar geometry with certain degree of distortion. The existence of tetrahedral coordination in metal complexes of Co^{2+}, Zn^{2+} and Cu^{2+} have also been documented with many other Schiff bases [41, 42].

Thermodynamic properties

In order to validate and to confirm unanimity of the stability constants, the thermodynamic properties of ML type complex species were calculated by semi-empirical method using PM6 parameters in the gas phase. The calculated thermodynamic properties (free energy, enthalpy, and entropy) of metal complexes are presented in Table 4. Each optimized structure had no imaginary frequency. Thermodynamic properties were calculated for ML species (M(II) = Co^{2+}, $Cu^{2+}$and Zn^{2+}) based on Eq. (4).

$$M(H_2O)_6 + LH_2 \longrightarrow ML + 6\,H_2O \qquad (4)$$

From the values of free energy change ΔG, which is calculated by applying equation $\Delta G = G_2 - G_1$ (G_2 = Free Energy of reactants and G_1 = Free energy of products), it is seen that the values are negative for all three metal complexes but, with a higher free energy change in case of Cu^{2+}, over Co^{2+} and Zn^{2+} ions, which attributes the ligands higher affinity for Cu^{2+} ions. Further, ΔG of metal complexes are in good agreement with the results obtained by experimental studies through potentiometry and spectrophotometry methods. The stability order Co^{2+} < Cu^{2+} > Zn^{2+} as obtained through experimental and theoretical methods, follows Irving William order [43].

CONCLUSIONS

The polyfunctional dipodal Schiff base, DOTA2HNAP exhibited an efficient metal-chelation with the divalent metal ions Co^{2+}, Cu^{2+} and Zn^{2+} through two N_2O_2 binding sites forming ML type complex. The trend of stability found for the complexes is in accord to Irving William order (Co^{2+} < Cu^{2+} > Zn^{2+}). Amide deprotonation of Cu^{2+}-L complex causes the formation of $CuLH_{-2}$ species whereas such deprotonation is not feasible

Table 4: Thermodynamic properties of ML (1:1) complexes (M = Co^{2+}, Cu^{2+}, Zn^{2+}) evaluated by semi-empirical /PM6 method.

Species	ΔH (kcal/mol)	ΔS (kcal/mol)	ΔG (kcal/mol)
[CoL]	-100.41	-0.08763	-74.30
[CuL]	-102.00	-0.08363	-77.08
[ZnL]	-100.82	-0.08663	-75.01

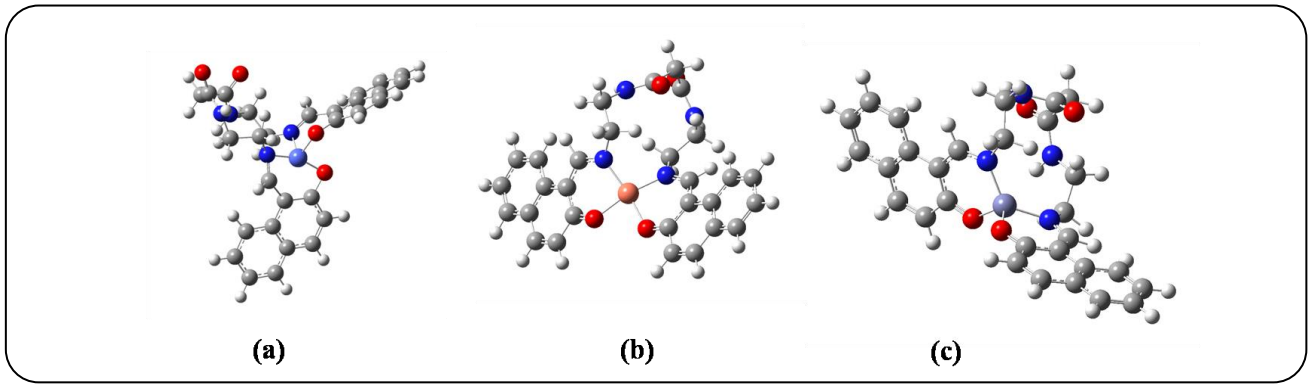

Fig. 12: Lowest energy structures of ML complexes (a) Co-L; (b) Cu-L; (c) Zn-L.

for Co^{2+} and Zn^{2+} metal complexes due to its endothermic nature that is not counterbalanced by ligand's effect. The naphthalene based dipodal chelator exhibited interesting photophysical properties. The change in absorption spectra of the ligand in an acidic pH (2-3) corresponds to the conversion of keto form to enol form, and shifting of absorption bands after pH ~ 5 implicates deprotonation of the chromophoric groups. The chelator showed fluorescence which is accompanied by the ESIPT mechanism. The fluorescence of the ligand was also found to be modulated with variation in pH. The intensity of the fluorescence emission of the ligand got diminished in the acidic and basic medium due to the existence of protonated –NH+/-OH and deprotonated -N/-O- forms as compared to its neutral form offering an OF-ON-OFF pH dependent molecular probe. However, a high fluorescence enhancement in the presence of Zn^{2+} ion at physiological pH, enables it to consider as noble fluorescence probe towards Zn^{2+} ions.

Acknowledgments

We are thankful to Department of Chemistry, National Institute of Technology, Kurukshetra and Central Instrumentation Facility of Panjab University, Chandigarh for supporting the research work.

Received : May 21, 2018 ; Accepted : Sep. 15. 2018

REFERENCES

[1] Mathews C.K., van Holde K.E., Ahern K.G., Enzymes: Biological Catalysts, In book *Biochemistry*, 3rd ed.; Roberts B., Weber L., Marsh J., Publication: Benjamin/ Cummings, San Fransisco, 391 (1999).

[2] Ngo Anh H., Bose Sohini, Do Loi H., Intracellular Chemistry: Integrating Molecular Inorganic Catalysts with Living Systems, *Chemistry - A European Journal*, **24**(42): 10584-10594 (2018).

[3] Ziyang H., Rongfeng Z., Peng R.C., Genetically Encoded Fluorescent Sensors for Measuring Transition and Heavy Metals in Biological Systems, *Current Opinion in Chemical Biology*, 4387-96 (2018).

[4] Badiye A., Kapoor N., Khajuria H., Copper Toxicity: A Comprehensive Study, *Res. J. Recent Sci.*, **2**: 58-67 (2013).

[5] Plum L.M., Rink L., Haase H., The Essential Toxin: Impact of Zinc on Human Health, *Int. J. Environ. Res. Public Health* **7**: 1342-1365 (2010).

[6] Mao X., Wong A.A., Crawford R.W., Cobalt Toxicity — an Emerging Clinical Problem in Patients with Metal-on-Metal Hip Prostheses? *MJA*, **194**: 649-651 (2011).

[7] Abu-Dief F.A., Ibrahim M.A., Mohamed A., Review on Versatile Applications of Transition Metal Complexes Incorporating Schiff Bases, *Beni-Suef University J. Basic App. Sci.*, **4**: 119 -133 (2015).

[8] Kumar G., Kumar D., Singh C.P., Kumar A., Rana V.B., Synthesis, Physical Characterization and Antimicrobial Activity of Trivalent Metal Schiff Base Complexes, *J. Serb. Chem. Soc.*, **75**(5): 629–637 (2010).

[9] Chang, E.L., Simmers C., Knight D.A., Cobalt Complexes as Antiviral and Antibacterial Agents. *Pharmaceuticals*, **3**: 1711-1728 (2010).

[10] Creaven B.S., Duff B., Egan D.A., Kavanagh K., Rosair G., Thangella V.R., Walsh M., Anticancer and Antifungal Activity of Copper(II) Complexes of Quinolin-2(1H)-one-Derived Schiff Bases, *Inorg. Chim. Acta*, **363**: 4048–4058 (2010).

[11] Antonov L., Fabian W.M.F., Nedeltcheva D., Kamounah F.S., Tautomerism of 2-Hydroxynaphthaldehyde Schiff Bases, *J. Chem. Soc. Perkin. Trans.*, **2**: 1173-1179 (2000).

[12] Abdullah M. Asiri A.M., Badahdah K.O., Khan S.A., g. Al-sehem A., s. Al-Amoudi M., Bukhari A.A., Spectroscopic Study and Semi-Empirical Calculations of Tautomeric Forms of Schiff Bases Derived from 2-Hydroxy-1-Naphthaldehyde and Substituted 2-Aminothiophene, *Org. Chem. Insights.*, **3**: 1–8 (2010).

[13] Furniss B.S., Hannaford A.J., Smith P.W.G., Tatchell A.R., "Vogel's Textbook of Practical Organic Chemistry", 5th ed., Longman Scientific & Technical, London, 131-234 (1989).

[14] Instruction Manual for Orion Star A111 pH meter Accompanied with Ross Ultra Combination pH Electrode 8102BNUWP of Thermo Scientific.

[15] Gan P., Sabatini A., Vacca A., Investigation of Equilibria in solution: Determination of Equilibrium Constants with the HYPERQUAD Suit Programs, *Talanta*, **53**: 1739 (1996).

[16] Alderighia L., Gans P., Ineco A., Peters D., Sabatini A., Vacca A., Hyperquad Simulation and Speciation (HySS): a Utility Program for the Investigation of Equilibria Involving Soluble and Partially Soluble Species, *Coord. Chem. Rev.*, **184**: 311 (1999).

[17] Gan P., Sabatini A., Vacca A., Determination of Equilibrium Constants from Spectrophotometric Data Obtained from Solutions of Known pH: The Program pHab, *Ann. Chim. (Rome)*, **89**: 45-49 (1999).

[18] Lee S., Rao B.A., Son Y.A., A Highly Selective Fluorescent Chemosensor for Hg^{2+} Based on a Squaraine–bis(rhodamine-B) Derivative. Part II, *Sensors and Actuators B*, **210**: 519–532 (2015).

[19] Bellamy L.J., "The Infra-red Spectra of Complex Molecules", 3rd ed., Chapman and Hall Ltd., London, (1975).

[20] Sahoo S.K., Muthu S.E., Baral M., Kanungo B.K., Potentiometric and Spectrophotometric Study of a New Dipodal Ligand N,N'-bis{2-[(2-hydroxybenzylidine) amino]ethyl}malonamide with Co(II), Ni(II), Cu(II) and Zn(II), *Spectrochim. Acta. A*, **63**: 574-586 (2006).

[21] Sosa J.M., Vinkovi´ M., c-Topi´ D.V., NMR Spectroscopyof 2-hydroxy-1-naphthylidene Schiff Bases with Chloroandhydroxy Substitutedaniline Moiety, *Croatica Chim. Acta*, **79**: 489–495 (2006).

[22] Dogan A., Sakyan I., Kilic E., Potentiometric Studies on Some α-Amino Acid- Schiff Bases and Their Manganese (III) Complexes in Dimethylsulfoxide-Water Mixtures at 25°C, *J. Sol. Chem.* **33**: 1539-1546 (2004).

[23] EI-Taher M.A., EI-Hatey M.T., Hussain T.M., Effect of Partially Aqueous Solutions of Different pH's on the Hydrolysis Rate of Some Schiff Bases. *Polish J. Chem.*, **75**: 79-91 (2001).

[24] Fabbirizzi L., Perotti A., Poggi A., The Deprotonated Amido vs. the Amino Group in the Stabilization of Coordinated Trivalent Copper and Nickel Cations. An Electrochemical Evaluation, *Inorg. Chem.*, **22**: 1411 (1983).

[25] Basoglu A., Parlayan S., Ocak M, Alp H., Halit K., Ozdemir M., Ocak U., Complexation of Metal Ions with the Novel 2-hydroxy-1-naphthaldehyde-derived Diamine Schiff Base Carrying a Macrobicyclic Moiety with $N_2O_2S_2$ Mxed Donor in Acetonitrile-Dichloromethane, *Polyhedron*, **28**: 1115-1120 (2009).

[26] Temel H., Cakir U., Otludil B,, Ugras H.I. Synthesis, Spectral and Biological Studies of Mn(II), Ni(II), Cu(II), and Zn(II) Complexes with a Tetradentate Schiff Base Ligand. Complexation Studies and the Determination of Stability Constants, *Synth. React. Inorg. Met.-Org. Chem.*, **31**: 1323-1337 (2001).

[27] Amar R.A.A., Abdel-Nasser M., Alaghaz A., Synthesis, Spectroscopic Characterization and Potentiometric Studies of a Tetradentate [N_2O_2] Schiff Base, N, N'-bis(2-hydroxybenzylidene)-1,1-Diaminoethane and Its Co (II), Ni(II), Cu(II) and Zn(II) Complexes, **8**: 8686-8699 (2013).

[28] Jung H.S., Verwilst P., Kim W.Y., Kim J.S., Fluorescent and Colorimetric Sensors for the Detection of Humidity or Water Content, *Chem. Soc. Rev.*, (2016). DOI: 10.1039/c5cs00494b.

[29] Zhao J., Ji S., Chen Y., Guo H., Yang P., Excited State Intramolecular Proton Transfer (ESIPT): from Principle Photophysics to the Development of new Chromophores and Applications in Fluorescent Molecular Probes and Luminescent Materials, *Phys. Chem. Chem. Phys.*, **14**: 8803–8817 (2012).

[30] Rodriguez-Cordoba W., Zugazagoitia J.S., Collado-Fregoso E., Peon J., Fluorescent Chemosensor Based on Schiff Base for Selective Detection of Zinc(II) in Aqueous Solution, *J. Phys. Chem. A*, **111**: 6241-6247 (2007).

[31] Li L., Dang Y.Q., Li H.W., Wang B., Wu Y., Fluorescent Chemosensor Based on Schiff Base for Selective Detection of zinc(II) in Aqueous Solution *Tetrahedron Lett.*, **51**: 618–621 (2010).

[32] Zhang M., Lu W., Zhou J., Du G., Jiang L., Ling J., Shen Z., A Simple and Effective Fluorescent Chemosensor for the Cascade Recognition of Zn 2þ and H_2PO_4 Ions in Protic Media, *Tetrahedron*, **70**: 1011-1015 (2014).

[33] Misra A., Shahid M., Dwivedi P., Srivastava P., Ali R., Razi S.S., A Simple Naphthalimide-Based Receptor for Selective Recognition of Fluoride Anion, *ARKIVOC*, 133-145 (2013).

[34] Sahana A., Banerjee A., Das S., Lohar S., Karak D., Sarkar B., Mukhopadhyay S.K., Mukherjee A.K., Das D., A Naphthalene-Based A^{l3+} Selective Fluorescent Sensor for Living Cell Imaging, *Org. Biomol. Chem.*, **9**: 5523 (2011).

[35] Singh N., Kaur N., Callan J.F., Incorporation of Siderophore Binding Sites in a Dipodal Fluorescent Sensor for Fe(III). *J. Fluoresc.*, **19**: 649–654 (2009).

[36] Li J., Yin C., Huo F., Development of Fluorescent Zinc Chemosensors Based on Various Fluorophores and Their Applications in Zinc Recognition, *Dyes and Pigments*, **131**: 100-133 (2016).

[37] Zhu H., Fan J., Wang B., Peng X., Fluorescent, MRI, and Colorimetric Chemical Sensors for the First-Row d-Block Metal Ions, *Chemical Society Reviews*, **44**(13): 4337-4366 (2015).

[38] Carter, Kyle P.; Young, Alexandra M.; Palmer, Amy E.; Fluorescent Sensors for Measuring Metal Ions in Living Systems; *Chemical Reviews*, 2014, 114(8), 4564-4601.

[39] Thiagarajany V., Ramamurthy P., Dual Fluorescence in a Schiff Base Derived from an Acridinedione Dye: Excited State Intramolecular Proton Transfer. *Bull. Chem. Soc. Jpn.*, **80**: 1307–1315 (2007).

[40] Roy P., Dhara K., Manassero M., Banerjee P., Synthesis, Characterization and Selective Fluorescent Zinc(II) Sensing Property of Three Schiff-Base Compounds, *Inorg. Chim. Acta*, **362**: 2927–2932 (2009).

[41] Costamagna J., Vargas J., Latorre R., Alvarado A., Mena G., Coordination Compounds of Copper, Nickel, Iron, with Schiff Bases Derived from Hydroxynaphthaldehyde and Salicylaldehyde, *Coord. Chem. Rev.*, **119**: 67-88 (1992).

[42] Hariharan M., Urbach F.L., The Stereochemistry of Tetradentate Schiff Base Complexes of Cobalt (II), *Inorg. Chem.*, **8**: 556-559 (1963).

[43] Irving H., Williams R.J.P., The Stability of Transition-Metal Complexes, *Inorganic Chemistry Laboratory*, *Oxford*, 3192-3210 (1952).

Please add Journal's name in Ref. [27] and Complete bibliographic data for Ref. [43]